



# Optimization of Jet Mixing Into a Rich, Reacting Crossflow

M.Y. Leong and G.S. Samuelsen  
University of California, Irvine, California

J.D. Holdeman  
Lewis Research Center, Cleveland, Ohio

## *The NASA STI Program Office ... in Profile*

Since its founding, NASA has been dedicated to the advancement of aeronautics and space science. The NASA Scientific and Technical Information (STI) Program Office plays a key part in helping NASA maintain this important role.

The NASA STI Program Office is operated by Langley Research Center, the lead center for NASA's scientific and technical information. The NASA STI Program Office provides access to the NASA STI Database, the largest collection of aeronautical and space science STI in the world. The Program Office is also NASA's institutional mechanism for disseminating the results of its research and development activities. These results are published by NASA in the NASA STI Report Series, which includes the following report types:

- **TECHNICAL PUBLICATION.** Reports of completed research or a major significant phase of research that present the results of NASA programs and include extensive data or theoretical analysis. Includes compilations of significant scientific and technical data and information deemed to be of continuing reference value. NASA counter-part of peer reviewed formal professional papers, but having less stringent limitations on manuscript length and extent of graphic presentations.
- **TECHNICAL MEMORANDUM.** Scientific and technical findings that are preliminary or of specialized interest, e.g., quick release reports, working papers, and bibliographies that contain minimal annotation. Does not contain extensive analysis.
- **CONTRACTOR REPORT.** Scientific and technical findings by NASA-sponsored contractors and grantees.
- **CONFERENCE PUBLICATION.** Collected papers from scientific and technical conferences, symposia, seminars, or other meetings sponsored or co-sponsored by NASA.
- **SPECIAL PUBLICATION.** Scientific, technical, or historical information from NASA programs, projects, and missions, often concerned with subjects having substantial public interest.
- **TECHNICAL TRANSLATION.** English-language translations of foreign scientific and technical material pertinent to NASA's mission.

Specialized services that help round out the STI Program Office's diverse offerings include creating custom thesauri, building customized databases, organizing and publishing research results ... even providing videos.

For more information about the NASA STI Program Office, you can:

- Access the NASA STI Program Home Page at <http://www.sti.nasa.gov/STI-homepage.html>
- E-mail your question via the Internet to [help@sti.nasa.gov](mailto:help@sti.nasa.gov)
- Fax your question to the NASA Access Help Desk at (301) 621-0134
- Phone the NASA Access Help Desk at (301) 621-0390
- Write to:  
NASA Access Help Desk  
NASA Center for Aerospace Information  
800 Elkridge Landing Road  
Linthicum Heights, MD 21090-2934



# Optimization of Jet Mixing Into a Rich, Reacting Crossflow

M.Y. Leong and G.S. Samuelsen  
University of California, Irvine, California

J.D. Holdeman  
Lewis Research Center, Cleveland, Ohio

Prepared for the  
36th Aerospace Sciences Meeting & Exhibit  
sponsored by the American Institute of Aeronautics and Astronautics  
Reno, Nevada, January 12–15, 1998

National Aeronautics and  
Space Administration

Lewis Research Center

## Acknowledgment

This work was supported by a grant from the NASA Lewis Research Center (Grant NAG3-1110).

### Available from

NASA Center for Aerospace Information  
800 Elkridge Landing Road  
Linthicum Heights, MD 21090-2934  
Price Code: A03

National Technical Information Service  
5287 Port Royal Road  
Springfield, VA 22100  
Price Code: A03

# OPTIMIZATION OF JET MIXING INTO A RICH, REACTING CROSSFLOW

M.Y. Leong\* and G.S. Samuelsen<sup>†</sup>  
 UCI Combustion Laboratory  
 University of California  
 Irvine, California 92697-3550

J.D. Holdeman<sup>‡</sup>  
 National Aeronautics and Space Administration  
 Lewis Research Center  
 Cleveland, Ohio 44135

## Abstract

Radial jet mixing of pure air into a fuel-rich, reacting crossflow confined to a cylindrical geometry is addressed with a focus on establishing an optimal jet orifice geometry. The purpose of this investigation was to determine the number of round holes that most effectively mixes the jets with the mainstream flow, and thereby minimizes the residence time of near-stoichiometric and unreacted packets. Such a condition might reduce pollutant formation in axially staged, gas turbine combustor systems. Five different configurations consisting of 8, 10, 12, 14, and 18 round holes are reported here. An optimum number of jet orifices is found for a jet-to-mainstream momentum-flux ratio ( $J$ ) of 57 and a mass-flow ratio ( $MR$ ) of 2.5. For this condition, the 14-orifice case produces the lowest spatial unmixedness and the most uniformly-distributed species concentrations and temperature profiles at a plane located one duct diameter length from the jet orifice inlet.

$n$  number of round holes in quick-mix module  
 $R$  radius of the quick-mix module  
 $r$  radial distance from the module center  
 $T_{jet}$  average jet air temperature  
 $T_{main}$  average mainstream temperature  
 $U_s$  spatial unmixedness  
 $V_{ref}$  reference velocity  
 $x$  axial distance from leading edge of orifice  
 $Y$  mass fraction of carbon  
 $\phi$  equivalence ratio =  $(fuel/air)_{local} / (fuel/air)_{stoichiometric}$

## Nomenclature

$DR$  jet-to-mainstream density ratio  
 $d$  orifice axial height, or round hole diameter  
 $f_{avg}$  average planar jet mixture fraction derived from carbon mass fraction  
 $f_{var}$  planar jet mixture fraction variance  
 $J$  jet-to-mainstream momentum-flux ratio =  $(\rho V^2)_{jets} / (\rho V^2)_{main}$   
 $MR$  jet-to-mainstream mass-flow ratio

## Introduction

Some processes involved in the injection of fuel and in the control of exhaust temperature rely on jet mixing with a crossflow of gas to mix streams of fluid. One particular application in which jet mixing in a crossflow plays a fundamental role is the Rich-burn/Quick-mix/Lean-burn (RQL) combustor. The success of this combustor in producing lower emissions than conventional gas turbine combustors depends on the effectiveness of the mixing section bridging the fuel-rich and fuel-lean stages of combustion. In this combustor design, the jets of air introduced into the quick-mix section should mix with the rich reacting crossflow as quickly as possible to bring the reaction to an overall lean equivalence ratio. It is

\*Graduate Researcher, Member.

<sup>†</sup>Professor, Corresponding Author, Associate Fellow.

<sup>‡</sup>Senior Research Engineer, Associate Fellow.

Copyright © 1998 by the American Institute of Aeronautics and Astronautics, Inc. No copyright is asserted in the United States under Title 17, U.S. Code. The U.S. Government has a royalty-free license to exercise all rights under the copyright claimed herein for Governmental Purposes. All other rights are reserved by the copyright owner.

hypothesized that mixing must occur in order to prevent the formation of hot pockets of fluid in the flow which in turn produce the high temperatures that drive pollutant formation.

A previous study by the authors<sup>1</sup> involved the construction of a facility which handled reacting tests in a cylindrical crossflow configuration. A particular jet orifice geometry, the 10 round hole case, was tested to explore the types of information that could be gathered from the experiment. The current study expands upon this initial work by addressing whether, for a given inlet condition, the orifice geometry can be optimized to mix pure air jets into a rich crossflow rapidly and uniformly to complete the reaction process.

### Background

Until recently, nonreacting experiments have been employed as a convenient tool to explore the mixing of air jets into a reactive cross stream. The primary goal of these studies was to determine orifice configurations that lead to optimal mixing within a specified duct length. In a cylindrical duct geometry, experimental surveys of the effect of the jet-to-crossflow momentum-flux ratio and the shape, orientation, and number of orifices on mixing have been performed in order to gain a mechanistic understanding of jet penetration and mixing dynamics.<sup>2</sup> A systematic optimization scheme on experimental data has been undertaken to determine the round hole configurations leading to optimal mixing at various momentum-flux ratios. For jet-to-mainstream momentum-flux ratios of 25 and 52, the number of round holes leading to optimal mixing have been 10 and 15, respectively.<sup>3</sup>

While extensive nonreacting jet mixing studies<sup>4-9</sup> have been performed, research into reacting flows has been limited. An initial reacting flow experiment studied the flowfield of a row of jets mixing with rich reacting gases confined to a cylindrical crossflow.<sup>1</sup> The work presented here continues the reacting flow investigation by using the diagnostic and analysis techniques developed in the previous study to determine an optimum round hole configuration. The objectives for this study are to obtain an orifice configuration leading to optimal mixing, and to determine a correlation between mixing and the achievement of desired outlet conditions.

### Experiment

#### Facility

The facility consists of a rich product generator and a jet-mixing section (Fig. 1). The rich product generator mixes propane gas with air upstream of the ignition point.

Combustion occurs in a zone stabilized by a swirler. To dissipate the swirl in the flow and to introduce a uniform nonswirling flow into the jet-mixing section, the rich product is passed through an oxide-bonded silicon carbide (OBSiC) ceramic foam matrix (Hi-Tech Ceramics) with a rated porosity of 10 pores/in.

The jet mixing section is comprised of a modular quartz section to which jet air is supplied from the surrounding plenum. The plenum is fed by four equally-spaced, individually-metered air ports located toward the base of the plenum. A high-temperature steel flow straightener installed in the plenum conditions and equally distributes the jet air entering the mixing module.

The quartz modules are 11 in. in length and have inner and outer wall diameters of 3.0 and 3.3 in. The row of orifices is positioned with its centerline 4.5 in. downstream from the module entrance. An alumina-silica blend of ceramic fiber paper provides sealing between the quartz module and the stainless steel mating surfaces. The modules tested were the 8-, 10-, 12-, 14-, and 18-orifice configurations. The 10-round hole module results were previously discussed in by Leong, *et al.*<sup>1</sup>

### Measurement Protocols

Temperature and species concentration data are obtained in a sector grid for six planes (Fig. 2(a)) for each module. With respect to the leading edge of the orifices, the planes are located:

Plane	Position	x/R
1	One module radius upstream	-1
2	Orifice leading edge	0
3	One-half of the orifice height	(d/2)/R
4	Orifice height	d/R
5	One module radius downstream	1
6	Two module radii downstream	2

Each planar grid consists of 16 points spread over a region that includes two orifices (Fig. 2(b)). The points include one point located at the center, and five points along each of the arc lengths of  $r/R = 1/3$ ,  $2/3$ , and 1. The points along each arc are distributed such that two points are aligned with the center of the orifices and three are aligned with the midpoint between orifice centers.

The same water-cooled probe is used for both temperature and species concentration measurements. For temperature measurements, a type B platinum-rhodium thermocouple is threaded through the sample extraction tube and positioned such that the junction extends 0.1 in.

beyond the probe tip. A computer program records and returns an average of 100 readings after a span of 20 sec.

Species concentration measurements are obtained by routing the sample through a heated line connected to the emission analyzers. Water is condensed from the gas before the sample is analyzed by nondispersed infrared (NDIR), paramagnetic, and flame ionization detection (FID). A data acquisition program reads 100 samples in 20 sec and returns an averaged quantity. The uncertainty in the analyzer measurement of the species concentration is 1 percent of the full scale reading.

The jet mixture fraction calculation is based on the carbon atom mass fraction, since carbon is conserved throughout the reaction. The carbon mass fractions are obtained by solving a system of equations using the species concentration data as inputs to obtain the wet mole fractions of the major combustion product species. The basic calculation procedure followed that outlined by Jones, *et al.*<sup>10</sup>

In order to determine the round hole configuration leading to the most uniform mixture of chemical species at the different planes, a normalized standard deviation parameter called spatial unmixedness  $U_S$  is used. The parameter is defined as

$$U_S = \frac{f_{\text{var}}}{f_{\text{avg}}(1 - f_{\text{avg}})} \quad (1)$$

where  $f_{\text{avg}}$  refers to the fully-mixed average jet mixture fraction value specific to each plane and  $f_{\text{var}}$  refers to the planar area-weighted variance deviating from  $f_{\text{avg}}$ .  $U_S$  values are bounded between 0 and 1, with the former corresponding to a perfectly mixed system and the latter referring to a totally unmixed system.<sup>9</sup>

TABLE I.—OPERATING CONDITIONS

Parameter	Value
Ambient pressure (atm)	1
Rich equivalence ratio $\phi$	1.66
Overall $\phi$	0.45
$T_{\text{main}}$ (°F)	2200
$T_{\text{jet}}$ (°F)	340
$V_{\text{ref}}$ (ft/sec)	60
Momentum-flux ratio J	57
Mass-flow ratio MR	2.5
Density ratio DR	3.3

The experiments are performed with jet-to-mainstream momentum-flux ratio J of 57. The total effective area of the mixing module orifices is 1.40 in.<sup>2</sup> The ratio of the total

effective jet area to cross-sectional area is 0.18. Operating conditions for the experiment are noted in table I.

## Results and Discussion

Measured temperature and species concentrations at the rich inlet crossflow Plane 1 showed near-uniform distributions for each module tested. The average temperature measured was 2200 °F with a 1 percent uncertainty, while the average concentrations of  $O_2$ , CO, and  $CO_2$  across all the modules were 0, 12.5, and 5.25 percent; respectively, with an 0.1 percent uncertainty. Because of the uniformity in the measured data, distributions at Plane 1 are not included in the figures showing the spatial evolution of the flowfield measurements.

### Jet Penetration and Reaction

**Temperature Profiles.** In combustor design, the attainment of a short combustor length is desired in order to maintain the compactness of the engine. For the RQL configuration, it is thus preferable to attain complete mixing within a minimal length. Non-reacting studies performed by Hatch, *et al.*<sup>2</sup> and Kroll, *et al.*<sup>3</sup> utilized a mixing length corresponding to one duct radius as an arbitrary reference plane of comparison. However, in initial reacting tests performed on the system,<sup>1</sup> it was shown that the reaction continues beyond the distance equivalent to one duct radius. Therefore, for the basis of this comparison between the five mixing modules, optimal mixing and reaction is determined within one duct diameter (or two duct radii) of the jet entrance (i.e., at Plane 6).

Figure 3 shows the evolution of temperature-related profiles for all the cases tested. The temperatures are normalized with respect to the area-weighted average value obtained at Plane 1 in the rich zone. Note that, because temperature is not a conserved scalar in a reacting flow, it is possible to attain temperatures that are greater than inlet values.

In each of the cases tested, cooler wall temperatures exist at the orifice leading edge at Plane 2. Heat loss occurs near the wall region as heat is transferred from the mixing module out through the wall, which is cooled by the air in the jet plenum feed. The jet fluid enters the module by Plane 3, which is positioned at the orifice center, and is denoted by the blue and green temperature bands representing cooler fluid in the flow.

By the orifice trailing edge at Plane 4, all the jet fluid has entered the crossflow. The range of higher normalized temperature bands above 1 is nearly absent in the 8 round

hole case as the jet fluid enters and disperses across the entire sector. Increasing the number of holes decreases the jet penetration and allows more of the reacting crossflow to pass through the center of the module.

Between the orifice region and the one radius mark at Plane 5, jet fluid mixing and reaction leads to a stratification of temperature ranges for all the modules. The occurrence of the lower temperature bands vary with respect to the number of orifices. The 8-orifice case shows green bands corresponding to 60 to 80 percent of the initial reaction temperature occurring in the core region. This trend is also present farther downstream at the two radii position at Plane 6, where the low normalized temperature range persists in the core. The 10-orifice case shows similar traits to the 8-orifice case, but to a lesser extent. In the 12-orifice case, temperatures across both Planes 5 and 6 range from 80 percent to over 100 percent of the initial temperatures. At Plane 6 the higher band of temperatures occurs along the wall region, as in the 8- and 10-orifice cases. On the other hand, the 14- and 18-orifice cases both yield lower temperature bands near the mid-radius at Plane 5. The subsequent mixing and reaction for the 14- and 18-orifice modules lead to a temperature distribution at Plane 6 in which the higher bands are located toward the core. The 14-orifice case also shows the persistence of a thin red higher temperature band at the wall.

Overall, the results show that increasing the number of orifices decreases the jet penetration. The 8-orifice case produces a case with jet overpenetration that results in a hot wall region and a cooler core region. The 10- and 12-orifice cases produce similar results that are less extreme than those from the 8-orifice case. The 14- and 18-orifice cases, however, produce a reverse stratified distribution of a hotter core region and a cooler wall region typical of jet underpenetration. Figure 4 illustrates this point with a plot of the axial profile of the centerline temperature ratios for each module. For all the modules, the centerline temperature remains nearly constant upstream of and in the immediate orifice region. Jet penetration to the centerline is indicated by a dip in the temperature relative to the initial rich reacting temperature. Jet overpenetration, denoted by the persisting presence of cooler jet fluid by Plane 5, can therefore be found in the 8-, 10-, and 12-orifice cases. The 14- and 18-orifice cases show centerline temperatures that are at or above their initial plane values and suggest either optimally-penetrating or underpenetrating jets. The number of round holes affects the degree of penetration: as the number of orifices is increased from 8 to 18, jet penetration transitions from over- to underpenetration.

Species Concentration Profiles. The effect of the number of orifices on jet penetration is also illustrated in the  $O_2$  distributions of Fig. 5. The jet trajectory can be defined by the locus of points showing maximal  $O_2$  concentration as a function of distance, since the mainstream contains no oxygen.

By the orifice trailing edge, all of the jet fluid should have entered and been accounted for in Plane 4. The sector cross-sections show a larger bulk of jet fluid occurring per orifice in the 8-orifice case and a successive decrease in bulk jet fluid per orifice as the number of orifices increases. This decrease in mass flow per orifice is attributed to the decrease in area per orifice, because the jet velocity through each orifice is constant for all five configurations. As the mass-flow of each jet decreases, the interaction between adjacent jets increases and jet penetration into the crossflow subsequently diminishes.

Plane 5 shows stratified  $O_2$  concentration distributions which give an indication of the jet mixing quality for each orifice configuration. For the overpenetrating 8-, 10-, and 12-round hole cases, reaction as seen by a decreased  $O_2$  concentration occurs beyond Plane 5 but is not as substantial as the further reaction that occurs beyond this plane for the underpenetrating 14- and 18-orifice cases.

High jet penetration causes fluid impingement at the centerline in the 8-orifice case and results in a large concentration of  $O_2$  in the central core. This condition confirms that the 8-orifice module is an overpenetrating case which is undesirable because the oxygen tends to accumulate in the center rather than disperse, mix, and react with the crossflow. Overpenetration also leads to less reaction since the accumulation of jet fluid in the center decreases the area of the jet-crossflow interface and consequently, the promotion of reactant interaction. The 10- and 12-orifice cases also exhibit overpenetration as the jet trajectory intersects with the centerline by Plane 6.

The 14- and 18-orifice cases produce jet trajectories that do not penetrate to the center by Plane 6. Without jet impingement, a more lateral spreading of jet fluid, as evidenced by the smaller range distribution of oxygen concentration values across the mixer radius, is achieved. As with jet overpenetration, jet underpenetration decreases the maximal jet-mainflow surface area of reaction because a portion of the jet fluid is bounded by the wall of the module. Jet underpenetration allows the rich reaction products to exit the module without completing the combustion process, which is undesirable. In the 14-orifice case, a larger jet surface area exposed to the crossflow



accelerates jet dispersion and reaction such that more of the rich mainstream flow reacts with rather than bypasses the jets. The 18-orifice case approaches an underpenetrating jet condition as more of the rich crossflow passes through the core region.

The experiment was designed to transition from a  $\phi = 1.66$ , fuel-rich section (Plane 1) to a  $\phi = 0.45$ , fuel-lean section (Planes 5 and 6). The equivalence ratio profiles in Fig. 6 serve as a guide in determining the extent to which the flow achieves the lean design condition. The crossflow entering at Plane 2 consists of a uniform rich flow at  $\phi = 1.60$ . By Plane 5, the equivalence ratios are distributed in stratified ranges. At this plane, the 8-, 10-, and 12-orifice cases show near-stoichiometric contours in the wake of the jets while the 14- and 18-orifice cases show rich effluent in the core. By Plane 6, the flowfields show the attainment of overall lean equivalence ratios for all cases. However, near-stoichiometric equivalence ratios between 0.9 and 1.0 occur along the wall for the 8-, 10-, and 12-orifice cases, and at the core for the 18-orifice case. Where the stoichiometric fuel-air equivalence ratios occur, corresponding regions of higher temperatures are found (refer to Fig. 3). Recall that higher temperatures occurred along the wall in the 8-, 10-, and 12-orifice cases and in the core for the 14- and 18-orifice cases. The transition from higher temperatures from the wall to the cylindrical crossflow core occurs between the 12- and 14-orifice cases.

#### Spatial Unmixedness

Figure 7 shows the planar spatial unmixedness  $U_S$  values derived from the jet mixture fractions at each plane. By Plane 4, which is positioned at the trailing edge of the orifices, all of the jet fluid has entered the crossflow, and the spatial unmixedness in the flowfield can be assessed. At this plane, the spatial unmixedness value varies between a low of 0.57 for the 8-orifice case and a high of 0.73 for the 12-orifice case. Downstream of the jet orifices, the subsequent mixing of the jets and the crossflow reduces the  $U_S$  values to levels under 0.20. At Plane 5, the 8-orifice module exhibits a spatial unmixedness value of 0.19 that is relatively higher than those for the rest of the modules. As the number of orifices increases from 12 to 18, the  $U_S$  values decrease from 0.14 to 0.12.

The  $U_S$  values show an overall reduction from the values in Plane 5, but the same trend in the relationship between the  $U_S$  values and the number of orifices seen in Plane 5 recurs in Plane 6. The 8-orifice module, with a  $U_S$  value of 0.11, continues to show a higher spatial unmixedness value than do the other cases. The spatial unmixedness continues to decrease as the number of orifices increases up until the 14-orifice case. For this configuration, the  $U_S$  value obtained is 0.026, which is

identical to the value calculated for the 18 orifice case. The spatial unmixedness values give an indication of the extent of mixing occurring between the rich crossflow and the air, but not of the degree of reaction between the two streams. From the temperature profiles in Fig. 3 and the equivalence ratio profiles in Fig. 6, it appears that somewhere between the 12 and the 14 round hole cases the most desired combination of lower overall temperatures and leaner equivalence ratio fields occurs. The 18-orifice case produces a low spatial unmixedness value because of the faster dilution of the jets, but the underpenetrating nature of the jets for this case causes a hot core of near stoichiometric reacting fluid to persist in the lean reaction region. Hence, of the 14 and 18 round hole cases showing the lowest  $U_S$  values, the 14-orifice case produces the optimal case of good overall mixing and reaction.

#### Optimum Number of Round Holes

For cylindrical crossflow geometries, several investigations have determined a jet penetration depth that leads to better mixing. In a numerical study performed by Talpallikar, *et al.*,<sup>11</sup> results suggest that optimal mixing occurs when the jet penetrates to the mid-radius. Kroll, *et al.*<sup>3</sup> infers from non-reacting experimental results that optimal mixing occurs when the jet penetrates to the radius that divides the mixer into an equal core and annular area, or at a radial distance 30 percent from the wall. For the cases tested, the jet trajectory (indicated by both oxygen and temperature profiles) intersects Plane 5: (1) beyond the midradius from the wall for the 8- and 10-orifice cases, (2) approaches but is beyond the mid-radius for the 12-orifice case, and (3) lies at a point before the mid-radius and toward the wall for the 14- and 18-orifice cases. The Talpallikar, *et al.* criterion supports the 12- or 14-orifice cases as candidates producing jet penetration that promotes the best mixing while Kroll, *et al.* data support the 14- or 18-orifice case as being the optimal configuration.

The number of round holes leading to optimal jet penetration can be predicted by an empirical relation developed for nonreacting jets injected into a subsonic cylindrical crossflow. The relation from Holdeman<sup>4</sup> suggests that the appropriate number of orifices  $n$  that will lead to optimal penetration may be determined by the following Eq. (2):

$$n = \frac{\pi\sqrt{2J}}{C} \quad (2)$$

where  $J$  is the jet-to-mainstream momentum-flux ratio, and  $C$  is an empirical constant that equal to 2.5 for optimal mixing of a single row of round holes. Note that this relation includes the assumption that the "optimum" spacing for a rectangular duct applies at the radius that

divides the can into equal-area cylindrical and annular sections.<sup>4</sup> In the reacting experiment where  $J = 57$ , the equation yields an optimal configuration of 13 orifices. This calculation corroborates the designation of the 14-orifice case as the optimal reacting case tested, but also suggests that distributions of an even higher, if not comparable, uniformity may be attained for a 13-orifice configuration.

Round hole optimization tests under nonreacting experiments show similar results. At a momentum-flux ratio of 52, Kroll, et al.<sup>3</sup> found that the 15 round hole case exhibited optimal mixing. However, the bracketing configurations tested in that experiment were the 12- and 18-orifice cases, which opens the possibility that the 13- or 14-orifice case may show more improved mixing. Nonetheless, the results show a possible correlation between the nonreacting and reacting tests that should be explored in future tests.

#### Summary and Conclusions

An experiment was performed to provide a test bed for the study of jet mixing in a uniform, nonswirling, rich reacting environment. In this demonstration, it was possible to compare the jet trajectory, reacting, and mixing processes for five round-hole configurations.

For a set momentum-flux ratio  $J = 57$  and mass-flow ratio  $MR = 2.5$  it was found (under atmospheric conditions) that:

- When jet penetration increases beyond optimal as in the 8-orifice case, the jet mass gravitates to and accumulates in the central core of the mixer rather than dispersing laterally throughout the radius of the mixer.
- When jet penetration decreases beyond the optimal point such as in the 18-orifice case, a hotter core of fluid bypasses the jet region without completing the reaction toward the desired fuel-lean state.
- The bulk of jet reaction and mixing occurs before the  $x/R = 1$  plane.
- Considering both mixing and completeness of reaction, the 14-orifice module, which exhibits jet trajectory penetration before the mixer half-radius, appears to be the best configuration tested. Good mixing and reaction leads to the attainment of a uniform mixture at the desired lean equivalence ratio. A goal of the mixing section is to achieve low

spatial unmixedness values as close to the orifice region as possible, although, as pointed out in Refs. 5 and 6, one must also peruse the corresponding distributions to avoid identifying an inappropriate choice as "best."

#### Acknowledgment

This work was supported by a grant from the NASA Lewis Research Center (Grant NAG3-1110).

#### References

1. Leong, M.Y., Samuelsen, G.S., and Holdeman, J.D. (1997). Mixing of Air Jets With a Fuel-Rich, Reacting Crossflow. Submitted to *Journal of Propulsion and Power* for publication review. (Also NASA TM-107430).
2. Hatch, M.S., Sowa, W.A., Samuelsen, G.S., and Holdeman, J.D. (1995). Jet Mixing into a Heated Cross Flow in a Cylindrical Duct: Influence of Geometry and Flow Variations. *Journal of Propulsion and Power*, **11**, pp. 393-402. (See also NASA TM-105390).
3. Kroll, J.T., Sowa, W.A., Samuelsen, G.S., and Holdeman, J.D. (1993). Optimization of Circular Orifice Jets Mixing into a Heated Cross Flow in a Cylindrical Duct. AIAA-93-0249 (Also NASA TM-105984).
4. Holdeman, J.D. (1993). Mixing of Multiple Jets with a Confined Subsonic Crossflow. *Prog. Energy Combust. Sci.*, v.19, pp. 31-70. (See also NASA TM-104412).
5. Holdeman, J.D., Liscinsky, D.S., Oechsle, V.L., Samuelsen, G.S., and Smith, C.E. (1996). Mixing of Multiple Jets With a Confined Subsonic Crossflow: Part I—Cylindrical Ducts. *Journal of Engineering for Gas Turbines and Power* (in press). (See also NASA-TM 107185)
6. Holdeman, J.D., Liscinsky, D.S., and Bain, D.B. (1997). Mixing of Multiple Jets With a Confined Subsonic Crossflow: Part II—Opposed Rows of Orifices in a Rectangular Duct. ASME-97-GT-439. (See also NASA TM-107461)
7. Zhu, G., Lai, M.C., and Lee, T. (1995). Penetration and Mixing of Radial Jets in Neck-Down Cylindrical Crossflow. *Journal of Propulsion and Power*, **11**, pp. 252-260.
8. Doerr, Th., Blomeyer, M., and Hennecke, D.K. (1997). Optimization of Multiple Jets Mixing With a Confined Crossflow. *Journal of Engineering for Gas Turbines and Power*, **119**, pp. 315-321.

9. Liscinsky, D.S., True, B., and Holdeman, J.D. (1993). Experimental Investigation of Crossflow Jet Mixing in a Rectangular Duct. AIAA-93-2037 (Also NASA TM-106152).
10. Jones, W.P., McDonell, V., McGuirk, J.J., Milosavljevic, V.D., Taylor, A.M.K.P., and Whitelaw, J.H. (1993). The Calculation of Mean Mixture Fractions in Turbulent Non-Premixed Methane Flames from Aspiration-Probe Measurements. Imperial College of Science, Technology and Medicine, Mechanical Engineering Department, Thermofluids Section Internal Report TFS/93/xx.
11. Talpallikar, M.V., Smith, C.E., Lai, M.C., and Holdeman, J.D. (1992). CFD Analysis of Jet Mixing in Low NO<sub>x</sub> Flametube Combustors. *Journal of Engineering for Gas Turbines and Power*, **114**, pp. 416-424. (Also NASA TM-104466).

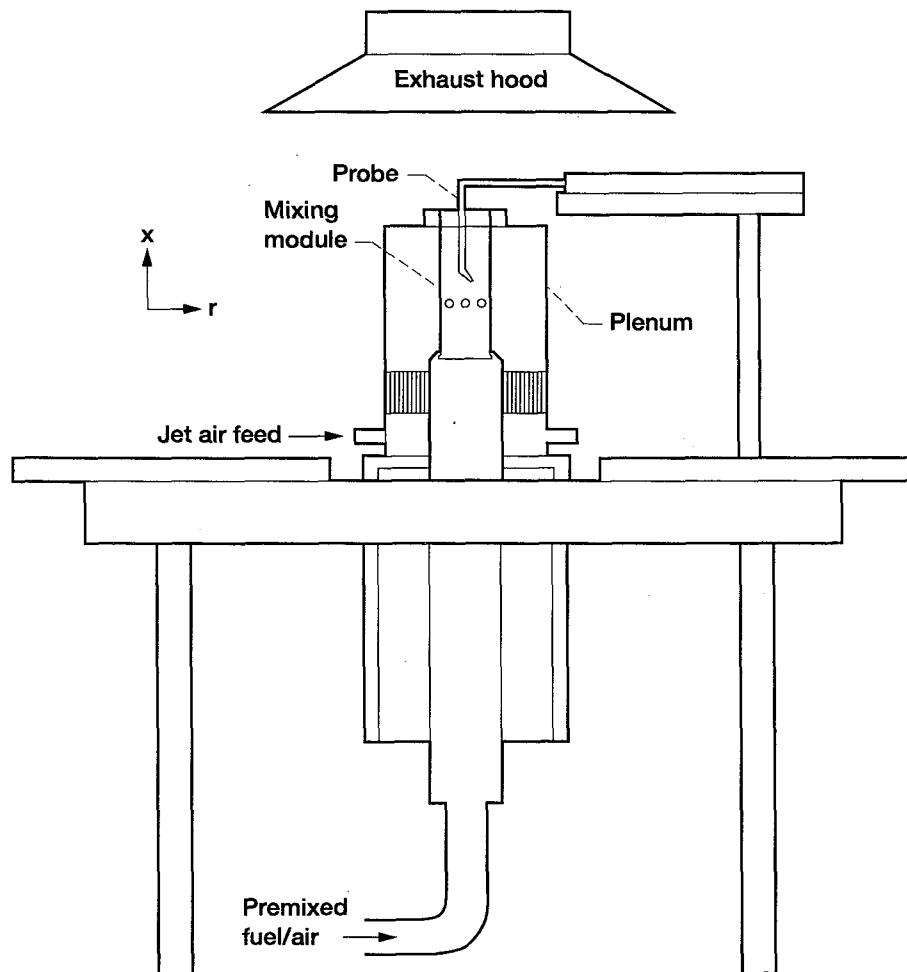


Figure 1.—Reacting flow test stand.

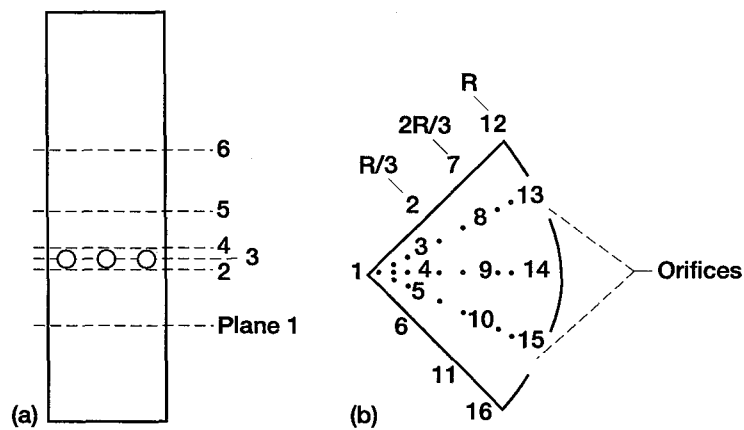


Figure 2.—Measurement locations. (a) Data plane locations. (b) Data point locations.

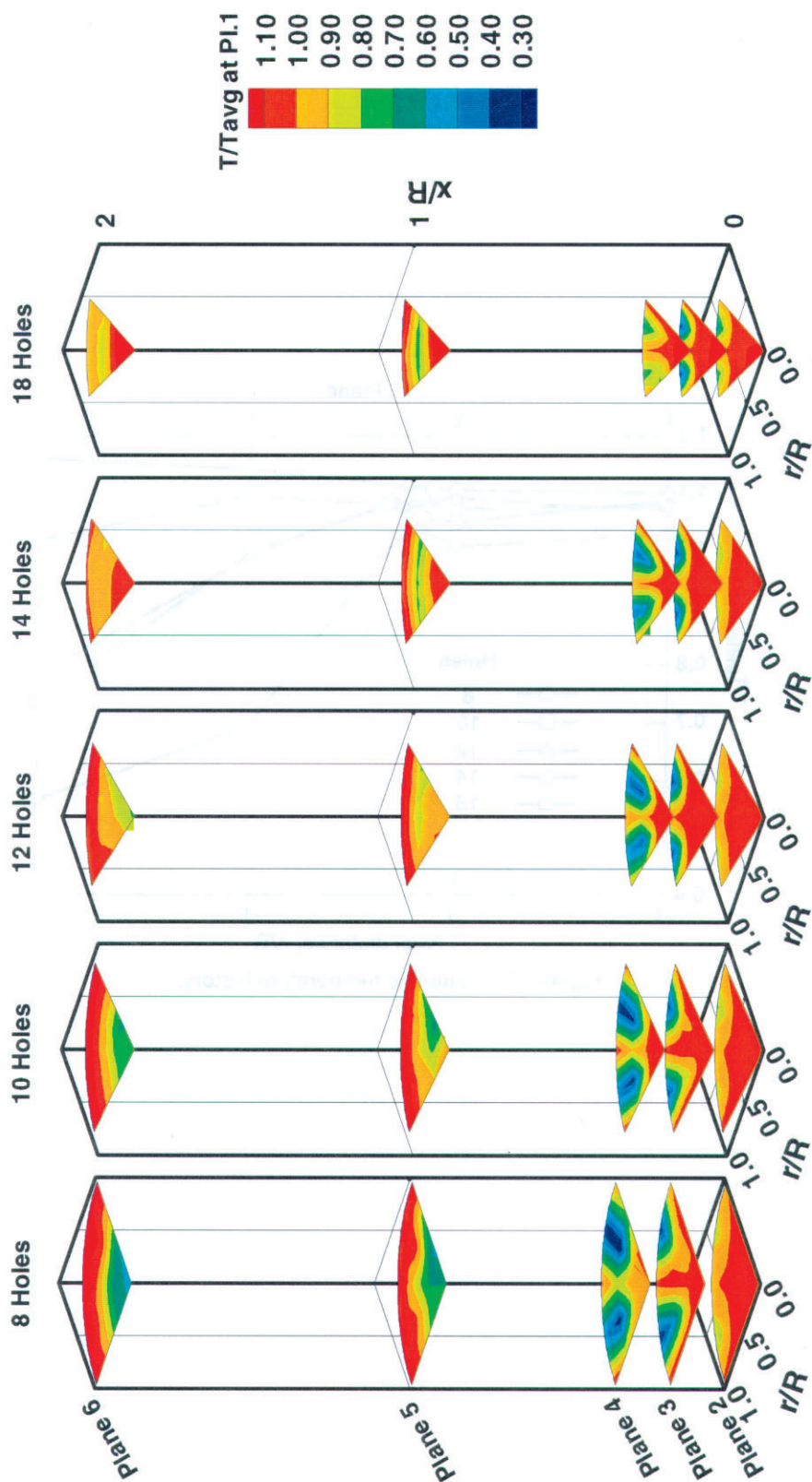


Figure 3.—Temperature profile comparison.

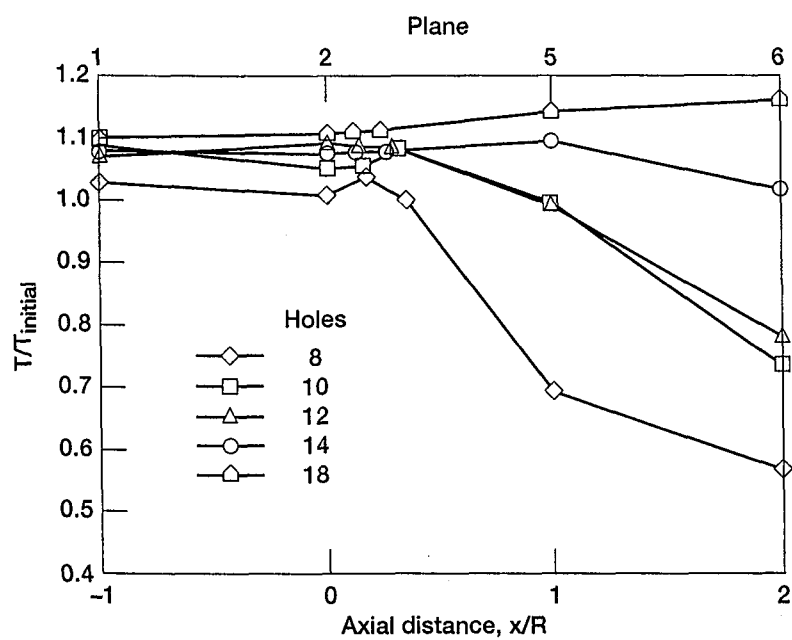


Figure 4.—Centerline temperature history.

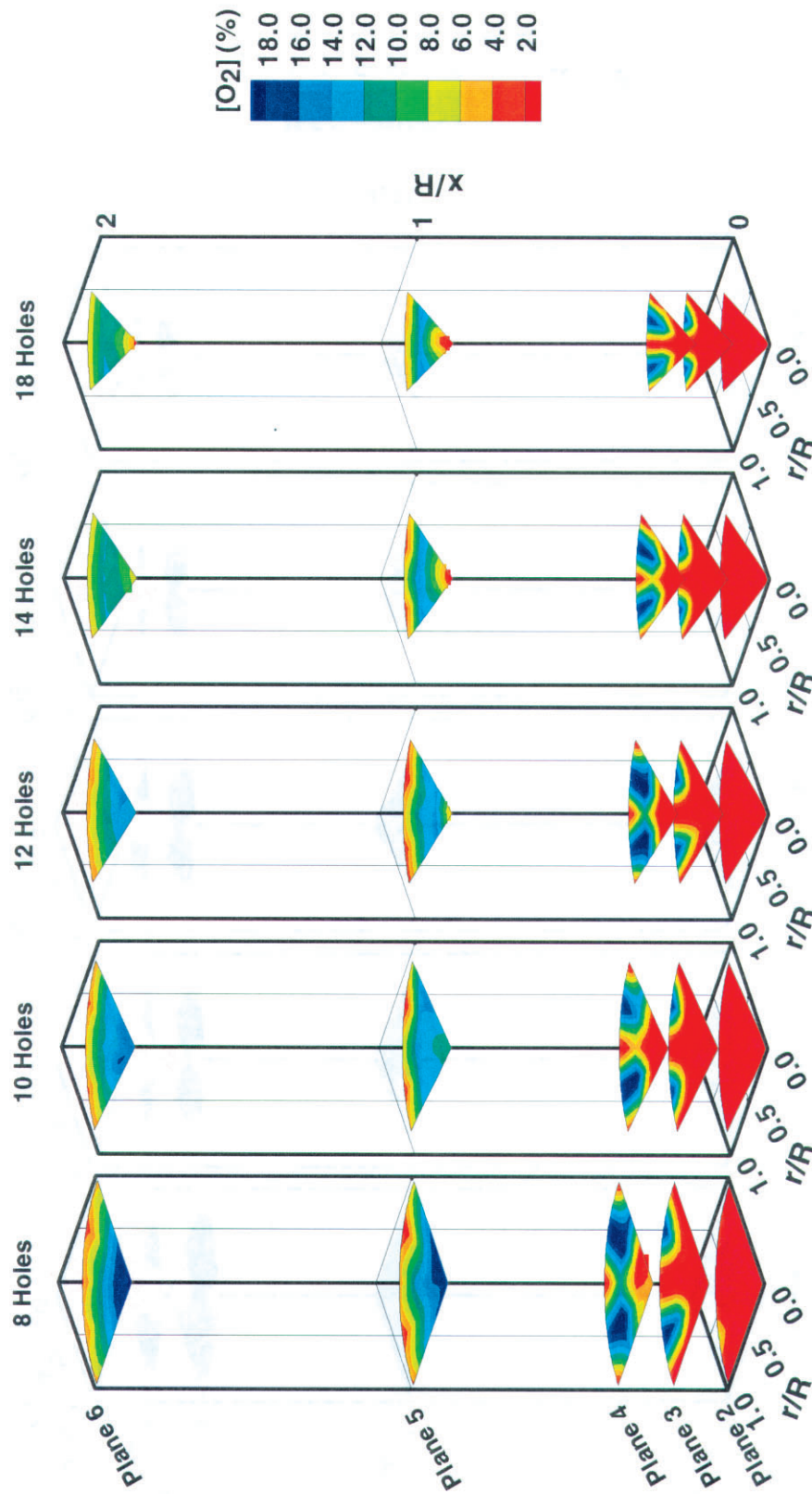


Figure 5.— $O_2$  profiles.

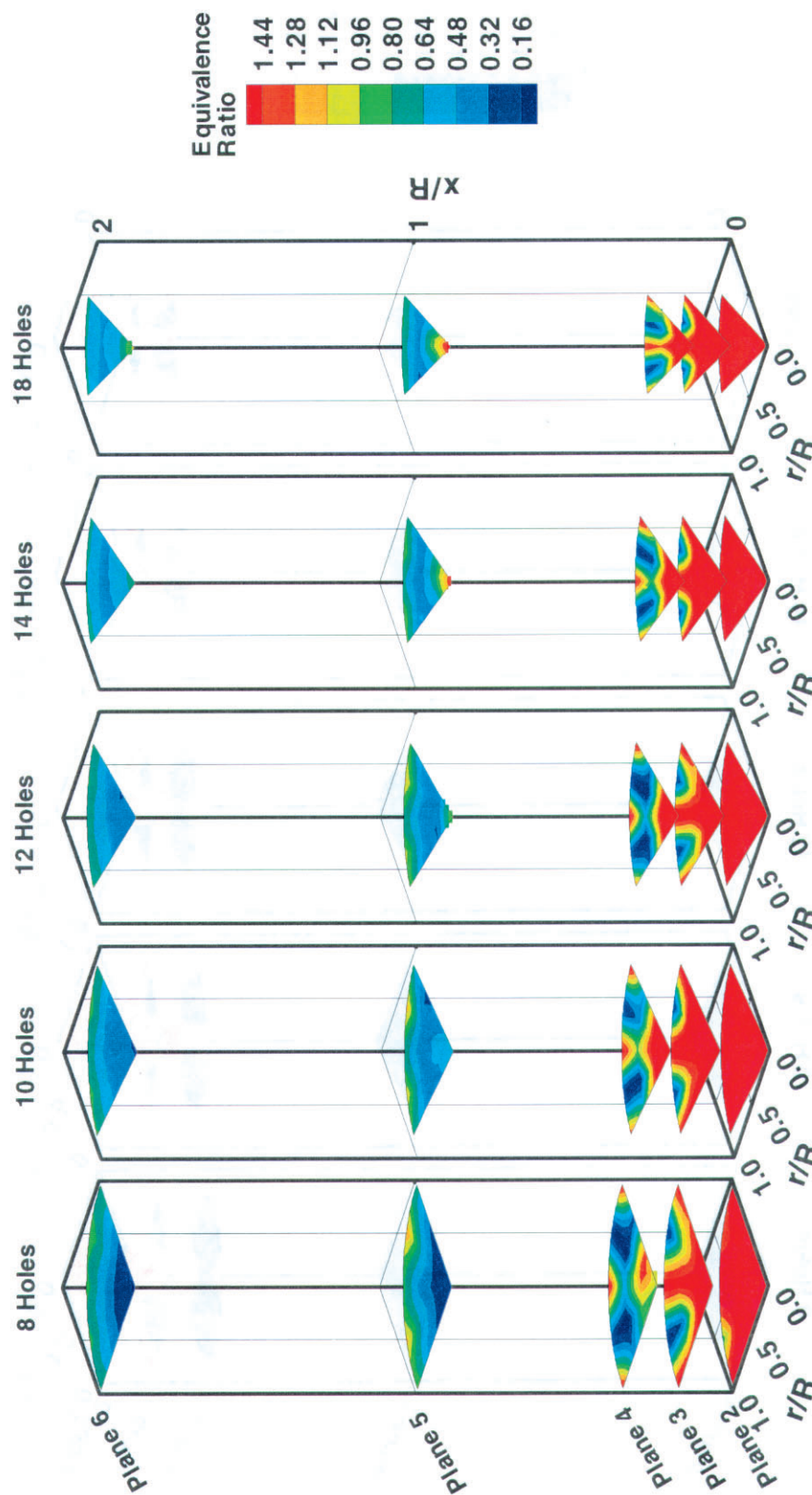


Figure 6.—Equivalence ratio profiles.



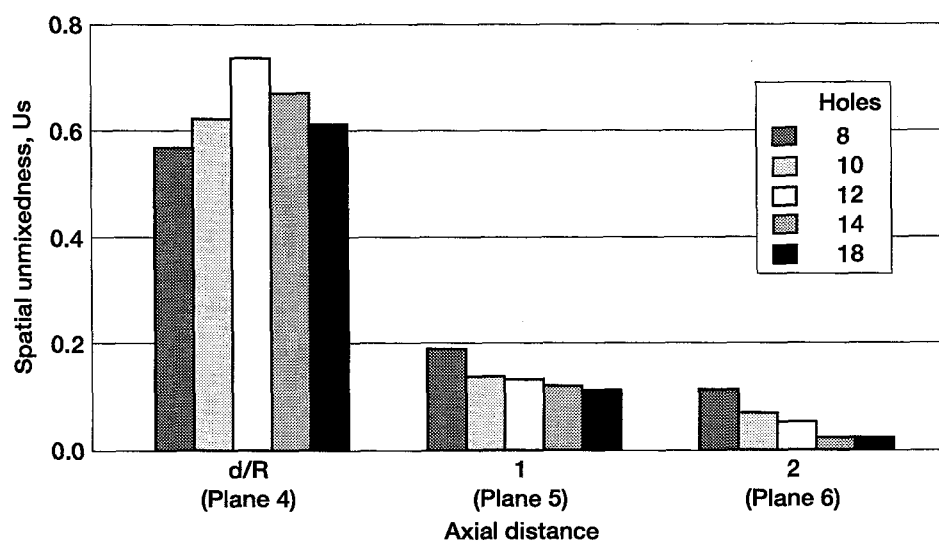


Figure 7.—Unmixedness values calculated per plane.

REPORT DOCUMENTATION PAGE			Form Approved OMB No. 0704-0188	
Public reporting burden for this collection of information is estimated to average 1 hour per response, including the time for reviewing instructions, searching existing data sources, gathering and maintaining the data needed, and completing and reviewing the collection of information. Send comments regarding this burden estimate or any other aspect of this collection of information, including suggestions for reducing this burden, to Washington Headquarters Services, Directorate for Information Operations and Reports, 1215 Jefferson Davis Highway, Suite 1204, Arlington, VA 22202-4302, and to the Office of Management and Budget, Paperwork Reduction Project (0704-0188), Washington, DC 20503.				
1. AGENCY USE ONLY (Leave blank)		2. REPORT DATE December 1997		3. REPORT TYPE AND DATES COVERED Technical Memorandum
4. TITLE AND SUBTITLE  Optimization of Jet Mixing Into a Rich, Reacting Crossflow			5. FUNDING NUMBERS  WU-537-02-20-00	
6. AUTHOR(S)  M.Y. Leong, G.S. Samuelsen, and J.D. Holdeman				
7. PERFORMING ORGANIZATION NAME(S) AND ADDRESS(ES)  National Aeronautics and Space Administration Lewis Research Center Cleveland, Ohio 44135-3191			8. PERFORMING ORGANIZATION REPORT NUMBER  E-10978	
9. SPONSORING/MONITORING AGENCY NAME(S) AND ADDRESS(ES)  National Aeronautics and Space Administration Washington, DC 20546-0001			10. SPONSORING/MONITORING AGENCY REPORT NUMBER  NASA TM-97-206294 AIAA-98-0156	
11. SUPPLEMENTARY NOTES  Prepared for the 36th Aerospace Sciences Meeting and Exhibit sponsored by the American Institute of Aeronautics and Astronautics, Reno, Nevada, January 12-15, 1998. M.Y. leong and G.S. Samuelsen, University of California, Irvine, California 92697-3550; J.D. Holdeman, NASA Lewis Research Center. Responsible person, J.D. Holdeman, organization code 5830, (216) 433-5846.				
12a. DISTRIBUTION/AVAILABILITY STATEMENT  Unclassified - Unlimited Subject Category: 07  Available electronically at <a href="http://gltrs.grc.nasa.gov/GLTRS">http://gltrs.grc.nasa.gov/GLTRS</a> This publication is available from the NASA Center for Aerospace Information, (301) 621-0390.			12b. DISTRIBUTION CODE	
13. ABSTRACT (Maximum 200 words)  Radial jet mixing of pure air into a fuel-rich, reacting crossflow confined to a cylindrical geometry is addressed with a focus on establishing an optimal jet orifice geometry. The purpose of this investigation was to determine the number of round holes that most effectively mixes the jets with the mainstream flow, and thereby minimizes the residence time of near-stoichiometric and unreacted packets. Such a condition might reduce pollutant formation in axially staged, gas turbine combustor systems. Five different configurations consisting of 8, 10, 12, 14, and 18 round holes are reported here. An optimum number of jet orifices is found for a jet-to-mainstream momentum-flux ratio (J) of 57 and a mass-flow ratio (MR) of 2.5. For this condition, the 14-orifice case produces the lowest spatial unmixedness and the most uniformly-distributed species concentrations and temperature profiles at a plane located one duct diameter length from the jet orifice islet.				
14. SUBJECT TERMS  Dilution jet mixing; Gas turbine; Combustion chamber; Emissions			15. NUMBER OF PAGES 19	
			16. PRICE CODE A03	
17. SECURITY CLASSIFICATION OF REPORT  Unclassified	18. SECURITY CLASSIFICATION OF THIS PAGE  Unclassified	19. SECURITY CLASSIFICATION OF ABSTRACT  Unclassified	20. LIMITATION OF ABSTRACT	